Revolution rather than rotation of AAA+ hexameric phi29 nanomotor for viral dsDNA packaging without coiling

Chad Schwartz[†], Gian Marco De Donatis[†], Hui Zhang[†], Huaming Fang[†], and Peixuan Guo*

Nanobiotechnology Center, Department of Pharmaceutical Sciences and Markey Cancer Center, University of Kentucky, Lexington, KY, 40536, USA

Running Title: ATPase riding along dsDNA

[†] Contributed Equally

*Address correspondence to:
Peixuan Guo, Ph. D.
William Farish Endowed Chair in Nanobiotechnology
School of Pharmacy, University of Kentucky
565 Biopharmaceutical Complex
789 S. Limestone Street
Lexington, KY 40536
Email: peixuan.guo@uky.edu
Phone : (859) 218-0128 (office); (513) 728-1411 (cell)

HIGHLIGHTS

- Phi29 DNA packaging motor use a revolution mechanism without rotation.
- DsDNA revolves unidirectionally using one strand along the hexameric channel wall.
- Motor revolves sequentially; only one ATP binds one ATPase subunit at any single time
- One ATP packages 1.75 base pairs (10.5 bp/turn ÷ 6ATP = 1.75 bp/ATP).
- Four lysine rings caused four steps of pause for the hexameric motor.

ABSTRACT

It has long been believed that the DNA-packaging motor of dsDNA viruses utilizes a rotation mechanism. Here we report a revolution rather than rotation mechanism for the bacteriophage Phi29 DNA packaging motor. Analogously, the Earth "rotates" along its own axis resulting in cycles of day and night; however, it "revolves" around the sun every 365 days. It has been found that the Phi29 motor contains six copies of the ATPase gp16 (Schwartz, De Donatis et al., 2013) (accompanying paper). ATP binding to one ATPase subunit stimulates the ATPase to adopt a conformation with a high affinity to bind dsDNA. ATP hydrolysis induces a new conformation with a lower affinity for dsDNA, thus pushing dsDNA away and transferring it to an adjacent subunit by a power stroke. DNA revolves unidirectionally along the hexameric channel wall, but neither the dsDNA nor the hexameric ATPase itself rotates. One ATP is hydrolyzed in each transitional step, and six ATPs are consumed for one helical turn of 360°. As demonstrated with Hill constant determination, binomial assay, cooperation and sequential analysis, transition of the same dsDNA chain along the channel wall, but at a location 60° different from the last contact, urges dsDNA to move forward 1.75 base pairs each step (10.5 bp/turn ÷ 6ATP = 1.75 bp/ATP). The 30°-tilted angle of each connector subunit that runs anti-parallel to the dsDNA helix facilitates the one-way traffic of dsDNA and coincides with the 12 subunits of the channel (360° ÷ 12 = 30°). The hexamer motor also caused four steps of pause due to the utilization of 4 lysine rings to facilitate the continuation of revolution (ACS Nano, conditionally accepted). Nature has evolved a clever machine to translocate DNA double helices that avoids the difficulties during rotation that are associated with DNA supercoiling. The discovery of the revolution mechanism might reconcile the stoichiometry discrepancy in many phage systems for which the ATPase was found to be present as tetramer, hexamer, and nonamers.

INTRODUCTION

The AAA+ (ATPases Associated with diverse cellular Activities) superfamily of proteins is a class of motor ATPases with a wide range of functions. Many members of this class of ATPases often fold into hexameric arrangements (Schwartz, De Donatis et al., 2013) (accompanying paper) (Wang, Mei et al., 2011;Grainge, Lesterlin et al., 2011;Kainov, Mancini et al., 2008;Mastrangelo, Hough et al., 1989;Egelman, Yu et al., 1995;Niedenzu, Roleke et al., 2001;Willows, Hansson et al., 2004) and are involved in DNA translocation, tracking, and riding (Mueller-Cajar, Stotz et al., 2011;Lowe, Ellonen et al., 2008;Parsons, Stasiak et al., 1995;Putnam, Clancy et al., 2001;Iyer, Leipe et al., 2004). Despite their functional diversity, the common characteristic of this family is their ability to convert chemical energy obtained from the hydrolysis of the γ-phosphate bond of ATP into a mechanical force, usually involving a conformational change of the AAA+ protein. This change of conformation generates both a loss of affinity for its substrate and a mechanical movement; which in turn is used to either make or break contacts between macromolecules, resulting in local or global protein unfolding, complex assembly or disassembly, or the translocation of DNA, RNA, proteins, or other macromolecules. These activities underlie processes critical to DNA repair, replication, recombination, chromosome segregation, DNA/RNA transportation, membrane sorting, cellular reorganization, and many others (Martin, Baker et al., 2005;Ammelburg, Frickey et al., 2006;Grainge, Bregu et al., 2007;Grainge, 2008;Lowe, Ellonen et al., 2008). Numerous biochemical and structural aspects of reactions catalyzed by AAA+ proteins have been elucidated, along with other interesting allosteric phenomena that occur during ATP hydrolysis. For instance, the crystal structure of the sliding clamp loader complex, a system that helps polymerases overcome the problem of torque generated during the extension of helical dsDNA, has revealed a spiral structure that strikingly correlates with the grooves of helical dsDNA; suggesting a simple explanation for how the loader/DNA helix interaction triggers ATP

hydrolysis, and how DNA is released from the sliding clamp (McNally, Bowman et al., 2010;Guenther, Onrust et al., 1997).

In both prokaryotic and eukaryotic cells, DNA needs to be transported from one cellular compartment to another. As for dsDNA viruses, they translocate their genomic DNA into preformed protein shells, termed procapsids, during replication (for review, see (Guo & Lee, 2007;Rao & Feiss, 2008;Zhang, Schwartz et al., 2012;Serwer, 2010)). This entropically unfavorable process is accomplished by a nanomotor that uses ATP as an energy source (Guo, Peterson et al., 1987b;Chemla, Aathavan et al., 2005;Hwang, Catalano et al., 1996;Sabanayagam, Oram et al., 2007;Schwartz, Fang et al., 2012;Lee, Zhang et al., 2008;Shu & Guo, 2003a;Chen & Guo, 1997). The dsDNA packaging motor also consists of a protein channel and two packaging molecules with which it carries out its activities. Our discovery 25 years ago has resulted in the knowledge that the larger molecule serves as part of the ATPase complex, and the smaller one is responsible for dsDNA binding and cleaving (Guo, Peterson et al., 1987b;Guo, Zhang et al., 1998); this notion has now become a well-established definition (for review, see (Guo & Lee, 2007;Rao & Feiss, 2008;Zhang, Schwartz et al., 2012;Serwer, 2010)). Besides the well-characterized connector channel core, the motor of bacterial virus phi29 involves an ATPase protein gp16 (Guo, Peterson et al., 1987b;Guo, Peterson et al., 1987a;Huang & Guo, 2003a;Huang & Guo, 2003b;Lee & Guo, 2006;Lee, Zhang et al., 2008;Ibarra, Valpuesta et al., 2001;Grimes & Anderson, 1990) and a hexameric packaging RNA ring (Guo, Zhang et al., 1998;Guo, Erickson et al., 1987;Shu, Zhang et al., 2007;Zhang, Endrizzi et al., 2012). The connector contains a central channel encircled by 12 copies of the protein gp10 that serves as a pathway for dsDNA translocation (Jimenez, Santisteban et al., 1986;Guasch, Pous et al., 2002;Badasso, Leiman et al., 2000).

The cellular components that show the strongest similarity to viral DNA packaging motor include FtsK, an AAA+ DNA motor protein that transports DNA and separates intertwined chromosomes during cell division (Iyer, Makarova et al., 2004), and the SpoIIIE family (Demarre,

Galli et al., 2013), an AAA+ protein responsible for transportation of DNA from a mother cell into the pre-spore during the cell division of Bacillus subtilis (Bath, Wu et al., 2000). It has recently been revealed that the ATPase of phi29 gp16 is similar to these families in structure and function (Iyer, Makarova et al., 2004;Guo, Zhang et al., 1998). Both the FtsK and SpoIIE DNA transportation systems rely on the assemblage of a hexameric machine. FtsK proteins contain three components: one for DNA translocation, one for controlling of orientation, and one for anchoring it to the substrate (Demarre, Galli et al., 2013). Extensive studies suggest that FtsK may employ a "rotary inchworm" mechanism to transport DNA (Massey, Mercogliano et al., 2006). The FtsK motor encircles dsDNA by a hexameric ring. During each cycle of ATP binding and hydrolysis within each FtsK subunit, one motif acts to tightly bind to the helix while the other progresses forward along the dsDNA. This process causes translational movement, a mechanism that is repeated by the subsequent transfer of the helix to the next adjacent subunit (Massey, Mercogliano et al., 2006). Many other hexameric dsDNA tracking motors function in a similar fashion, including TrwB, which is used in DNA transport during bacterial conjugation (Gomis-Ruth, Moncalian et al., 2001); Rad54, an ATPase supporting viral DNA replication (Amitani, Baskin et al., 2006); and RuvB that plays a role in the resolution of the Holliday junction during homologous recombination (Chen, Yu et al., 2002).

Many intriguing packaging models have been proposed for the motor of dsDNA viruses (Serwer, 2010;Maluf, Gaussier et al., 2006;Yu, Moffitt et al., 2010;Moffitt, Chemla et al., 2009;Aathavan, Politzer et al., 2009). It has long been popularly believed that viral DNA packaging motors run through a rotation mechanism involving a five-fold/six fold mismatch structure (Hendrix, 1978). The best-studied bacteriophage Phi29 DNA packaging motor was constructed in 1986 (Guo, Grimes et al., 1986) and has been shown to contain three co-axial rings (Fig. 1) (Guo, Peterson et al., 1987b;Guo, Erickson et al., 1987;Lee & Guo, 2006;Ibarra, Valpuesta et al., 2001). In 1987, an RNA component was discovered on the packaging motor (Guo, Erickson et al., 1987), and subsequently, in

1998, this RNA particle was determined to exist as a hexameric ring (Guo, Zhang et al., 1998;Zhang, Lemieux et al., 1998) (featured by *Cell* (Hendrix, 1998)). Based on this structure, it was proposed that the mechanism of the Phi29 viral DNA packaging motor is similar to that used by other hexameric DNA tracking motors of the AAA+ family (Guo, Zhang et al., 1998). This notion has caused a fervent debate concerning whether the RNA and ATPase of the motor exist as hexamers or as pentamers. Many laboratories have persisted to prove the pentameric model (Chistol, Liu et al., 2012;Yu, Moffitt et al., 2010;Morais, Koti et al., 2008), despite the solid finding of the presence of hexameric folds in the motor, as revealed by biochemical analysis (Schwartz, De Donatis et al., 2013) (accompanying paper) (Guo, Zhang et al., 1998;Zhang, Lemieux et al., 1998;Hendrix, 1998); single molecule photobleaching (Shu, Zhang et al., 2007); gold labeling imaged by EM (Xiao, Zhang et al., 2008;Moll & Guo, 2007;Shu, Zhang et al., 2007); nano-fabrication (Xiao, Demeler et al., 2010); and RNA crystal structure (Zhang, Endrizzi et al., 2012). Due to strong supporting data in favor of the motor hexamer, the pentamer-supporters have proposed alternatives to reconcile the pentamer and hexamer debate. One theory is that a pRNA hexamer is first assembled on the motor, after which one of the subunits leaves, resulting in the final pentameric state (Morais, Tao Y et al., 2001;Simpson, Tao et al., 2000;Morais, Koti et al., 2008). This proposition was countered by findings showing that the motor intermediates isolated during the active DNA packaging process also contain a hexamer (Shu, Zhang et al., 2007). Due to the discrepancy in their data, another group proposed an alternative theory in which one of the subunits in the pentamer ring is inactive during each cycle and the other four pentamer subunits function sequentially during the DNA packaging process (Moffitt, Chemla et al., 2009;Yu, Moffitt et al., 2010). In the accompanying paper, we provide conclusive data that confirms that the ATPase motor is in fact a hexamer (Schwartz, De Donatis et al., 2013), that it is a relative of the hexameric AAA+ DNA translocase, and that the motor mechanism of DNA translocation involves revolution without a counter force, rather than a rotational mechanism that involves a coiling force, as has been popularly

believed. For details, please view four mechanism animations and one real-time observation movie at http://nanobio.uky.edu/movie.html, using Internet Explorer or Chrome.

MATERIALS AND METHODS

Cloning, mutagenesis and protein purification.

The engineering of eGFP-gp16 and the purification of gp16 fusion protein have been reported previously (Lee, Zhang et al., 2009). eGFP-gp16 mutants G27D, E119A, R146A, and D118E E119D were constructed by introducing mutations to the gp16 gene (Keyclone Technologies).

Measurement of gp16 ATPase activity.

Enzymatic activity *via* fluorescence was described previously (Lee, Zhang et al., 2008).

In Vitro virion assembly assay

Purified *in vitro* components were mixed and subjected to virion assembly assay, as previously described (Lee & Guo, 1994).

Statistical analysis and data plotting.

Most statistical analysis was performed using Sigmaplot 11. Determination of the Hill coefficient was obtained by nonlinear regression fitting of the experimental data to the following equation: $E= E_{max}*(x)^n/(k_{app} +(x)^n)$, where E and E_{max} refer to the concentration of gp16/DNA complex, X is the concentration of ATP or ADP, K_{app} is the apparent binding constant, and n is the Hill coefficient.

CE experiments to determine ratio of gp16 to bound dsDNA:

CE (Capillary electrophoresis) experiments were performed on a Beckman MDQ system equipped with double fluorescent detectors (488nm and 635nm excitation). The capillary used was a bare borosilicate capillary 60 cm in total length and a 50 μm inner section. The method consisted of a 20 min separation at 30 KV normal polarity. Typical assay conditions contained 50 mM Tris-HCl, 100 mM borate at pH 8.00, 5 mM $MgCl_2$, 10% PEG 8000 (w/v), 0.5% acetone (v/v), 3 μM eGFP-gp16 monomer and variable amounts of ATP/ADP and DNA.

Sucrose gradient sedimentation of gp16/prohead:

Ultra-pure proheads were incubated with eGFP-gp16 and pRNA at room temperature for an extended period. The samples were loaded on top of a 5-20% sucrose gradient dissolved in buffer that mimicked *in vivo* conditions; 200 μl 60% sucrose was used as a cushion. The samples were then sedimented at 35000 rpm for 4 hr, fractionated, and the fluorescent signal was captured using a Synergy IV microplate reader.

Electrophoretic Mobility Shift Assay (EMSA):

The engineering of eGFP-gp16 and the purification of gp16 fusion protein (Lee, Zhang et al., 2009), as well as the gp16 and dsDNA binding assay (Schwartz, Fang et al., 2012), have been reported previously. Cy3- or Cy5-dsDNA (40 bp) was prepared by annealing two complementary DNA oligos containing Cy3 or Cy5 labels at their 5' ends (IDT). The annealed product was purified from 10% polyacrylamide gel. The samples for EMSA assay were prepared in 20 μl buffer A (20 mM Tris-HCl, 50 mM NaCl, 1.5% glycerol, 0.1 mM Mg^{2+}). 1.78 μM eGFP-gp16 was mixed with 7.5 ng/μl 40bp Cy3-DNA at various conditions in the typical fashion. The samples were incubated at ambient temperature for 20 min and then loaded onto a 1% agarose gel (44.5 mM Tris, 44.5mM boric acid) for

electrophoresis for 1 hr under 80 V at 4°C. The eGFP-gp16 and Cy3-DNA in the gel was analyzed by fluorescent LightTools Whole Body Imager using 488 nm and 540 nm excitation wavelengths for GFP and Cy3, respectively.

Observation of gp16 motion:

Double-stranded lambda DNA (48kbp) was stretched by forming a tightrope between two polylysine coated silica beads (Kad, Wang et al., 2010). The dsDNA was tethered between beads by back-and-forth infusion of DNA over the beads for 10 min; the tethering was formed as a result of charge-charge interactions. The stretched DNA chain was lifted above the surface by the 4 μm silica beads. The incident angle of the excitation beam in objective-type TIRF (total internal reflection fluorescence) was adjusted to a sub-critical angle in order to image the samples a few microns above the surface with low fluorescence background (Kad, Wang et al., 2010). To-Pro-3 was used to confirm the formation of the DNA tightropes. After the DNA tightrope was formed, a mixture of 1 nM Cy3-gp16 with 100 nM unlabeled gp16 in buffer B (25 mM Tris, pH 6.1, 25 mM NaCl, 0.25 mM $MgCl_2$) was infused into the sample chamber for binding to the stretched DNA. After 30 min incubation, a solution containing anti-photobleaching mixture (Shu, Zhang et al., 2007) was infused into the chamber to detect binding. Movies were taken after the chamber was washed with buffer C (25 mM Tris, pH 8, 25 mM NaCl, 0.25 mM $MgCl_2$). A comparison was made of washings with buffer C, with and without 20 mM ATP. Sequential images were acquired with a 0.2 sec exposure time at an interval of 0.22 sec, with a laser of 532 nm for excitation. The movies were taken for about 8 min, or until the Cy3 fluorophores lost their fluorescence due to photobleaching. Image J software was utilized to generate kymographs to show the displacement of the Cy3-gp16 spots along the DNA chains.

RESULTS

The structure of the hexameric motor

The essential components of the Phi29 DNA packaging motor include the dodecameric channel (also known as the connector) and the ATPase gp16 geared by a ring of RNA. The crystal structure of the three-way junction (3WJ) of the pRNA (Shu, Shu et al., 2011), one of the motor components, has recently been solved (Zhang, Endrizzi et al., 2012) and the hexameric pRNA ring has been constructed (Fig. 1A). AFM images revealed an elaborate, ring-shaped structure consisting of six distinct arms representing the six subunits of pRNA (Fig 1D).

Sliding of gp16 out of dsDNA verified by addition of steric blocks to the end of dsDNA

When Cy3-dsDNA was mixed with eGFP-gp16, a transfer of energy from the donor fluorophore (eGFP) to the acceptor fluorophore (Cy3) was observed, indicating that the protein fluorophore is at a close proximity to the dsDNA fluorophore. However, after addition of ATP, the Förster Resonance Energy Transfer (FRET) efficiency decreased significantly (Fig. 2), suggesting that the protein had walked off of the DNA after ATP hydrolysis. In contrast, the binding of gp16 to dsDNA was significantly enhanced in the presence of non-hydrolyzable ATP analogue, γ-S-ATP, as shown in both gel shift and binding assays. These data support our recent report that ATP induces a conformational change in gp16 resulting in a higher binding affinity for dsDNA (Schwartz, Fang et al., 2012). To further verify whether the discharge of gp16 from DNA is simple dissociation or a process by which gp16 walks along DNA, we exploited a streptavidin hindrance test (Fig. 3). Two biotin moieties were conjugated to the 3'-ends of the two strands of the dsDNA (Fig. 3). The terminally biotinylated DNA was incubated with streptavidin, which binds to biotin and provides a blockade for gp16's departure. If gp16 dissociates from the DNA such that binding is an "on and off" manner, instead of tracking or walking along DNA, streptavidin would not be able to block the gp16 discharge

and would essentially render the addition of the streptavidin useless. However, if gp16 formed a ring and slid along the dsDNA helix, streptavidin will effectively block the departure of gp16 from dsDNA. Our results revealed that the gp16/DNA/γ-S-ATP complexes remained stable in the presence of ATP when the terminally biotinylated Cy3 DNA was pre-incubated with streptavidin, but binding was not retained in the presence of ATP and absence of streptavidin.

Binomial quantification assay revealing one Walker B mutant completely blocks motor function

The Walker A motif of AAA+ proteins has previously been shown to be responsible for ATP binding, and the Walker B motif the initiation of ATP hydrolysis (Story & Steitz, 1992). The Walker A motif has previously been identified in Phi29 ATPase gp16 (Guo, Peterson et al., 1987b) and recently we have confirmed the presence of the Walker B motif in gp16 by introducing mutation to both motifs and performing functional assays (Schwartz et. al., Virology, Accompanying paper). With the cloned mutants to the Walker B motif, the Hill constant was evaluated using capillary electrophoresis of DNA binding affinity to distinguish between a sequential or concerted action mechanism.

In order to elucidate the mechanism of the DNA packaging motor, we had to empirically determine the number of copies of inactive Walker B mutant within the hexameric ring that are required to block the entire DNA packaging process. This will partially explain whether the action of motor component is sequential or concerted. The minimum number (y) of mutant gp16 needed to block the packaging within the hexameric ring was predicted with the equation $(p+q)^6 = \binom{6}{0}p^6 + \binom{6}{1}p^5q^1 + \binom{6}{2}p^4q^2 + \binom{6}{3}p^3q^3 + \binom{6}{4}p^2q^4 + \binom{6}{5}p^1q^5 + \binom{6}{6}q^6$, where p and q represent the ratio of wildtype and Walker B mutant gp16, respectively, and p + q = 1 (Fig. 4). Using this expanded binomial, each term represented a different mixed hexamer where the exponents of p and q were indicative of the copy numbers of wildtype and mutant in each mixed hexamer, respectively. For

example, the term $\binom{6}{3}p^3q^3$ indicates that the hexameric gp16 contains a perfect mix of 3 wildtype and 3 Walker B mutant monomers. Our empirical data almost perfectly overlapped with the theoretical curve corresponding to the term $\binom{6}{0}p^6q^0$, indicating that when y is greater than or equal to 1, the entire complex becomes inactive, suggesting that one copy of the Walker B mutant is capable of completely abolishing motor activity.

Motor ATPase tightly clinched dsDNA after binding to ATP and subsequently pushed the dsDNA away after ATP hydrolysis

Similar to the AAA+ motor proteins that undergo a cycle of conformational changes during their interaction with ATP and adaptation of two distinct states, Phi29 motor ATPase also exists in either a high or low affinity for the DNA substrate. Recently, it has been qualitatively demonstrated *via* electrophoretic mobility shift assays (EMSA) (Schwartz, Fang et al., 2012) that the motor ATPase gp16's affinity towards dsDNA increases in the presence of γ -s-ATP, but remains low in the presence of ADP, AMP, or no nucleotide. To get quantitative information about the different binding states of gp16, we utilized a CE assay that allowed for direct quantification of the amount of DNA bound to gp16. At increasing concentrations of γ -s-ATP, the amount of bound DNA increased progressively, indicating that gp16 transitioned from a state in which binding to DNA was unfavorable to one in which binding was preferred (Fig. 5A). The regression plot of dissociation constant (K_d) for dsDNA versus concentration of γ -s-ATP indicated that the affinity of gp16 for substrate increased 40 fold in saturating amounts of γ -s-ATP (Fig. 5B). This significant increase strongly suggests that the species that binds to DNA is the gp16-ATP complex and the gp16 binds first to ATP and secondly to DNA, as also suggested in the previous report (Schwartz, Fang et al., 2012). However, adding ADP, even at non-physiological conditions (up to 6 mM), failed to promote an increase in dsDNA binding affinity (Fig.

5C). Furthermore, the amount of DNA bound to g16 was comparable to the situation in which no nucleotide was added. These observations indicate that gp16 cycles through states of ATP binding/DNA loading and ATP hydrolysis/DNA release or pushing. The conclusion was also supported by the finding that addition of normal ATP to the gp16/DNA/γ-s-ATP complex promoted the departure of the dsDNA from the complex (Fig. 7, and accompanying paper).

Only one molecule of ATP is sufficient to generate the high affinity state for DNA in the ring of the motor ATPase.

Next, we sought the answer to how many nucleotides were required for gp16 to generate the high affinity state for dsDNA; in other words, how many subunits need to bind to ATP in order for the gp16 hexamer to stably associate to dsDNA. This information is useful to understand how the hexameric complex of gp16 utilizes the substrate in order to generate unidirectional DNA translocation. AAA+ proteins are typically organized into a homo-oligomeric assembly where each component contains the recognition motifs required for binding of the substrate. In principle, one can imagine that each subunit can bind to the substrate independently from the others; however, such an arrangement can lead to futile cycles of ATP consumption. Two major configurations can be hypothesized to avoid the above described scenario. Firstly, it may be possible that the binding sites for the substrate consist of the same recognition motifs in all the subunits, and in this case, all subunits can bind at the same time to the substrate. In this hypothetical situation, it is intuitive to imagine that a form of coordination among the subunits must also exist at the level of ATP hydrolysis, since the most effective mechanism of translocation would allow all subunits to hydrolyze at the same time corresponding to an exodus of the dsDNA substrate. The second possibility is that DNA is bound at any given time to only one subunit of the oligomer, and after the cycle of ATP hydrolysis is terminated in the specific subunit that binds DNA, the substrate is then passed to the next subunit in the high ATP affinity state in order to

initiate another cycle of hydrolysis. To distinguish between these two scenarios, we analyzed the amount of DNA bound to gp16 by keeping the concentration of gp16 and DNA constant and varying the concentration of γ-s-ATP in the reaction mixture (Fig. 5D). If more than one γ-s-ATP per oligomer of gp16 is required to generate the high affinity state for DNA in the protein, the plot would show a cooperativity profile, with the Hill coefficient representing the amount of γ-s-ATP required to be bound to gp16. Our data exhibits no cooperativity in binding (Hill coefficient = 1.5) indicating that all of the subunits of gp16 are not required to be bound to γ-s-ATP to stabilize binding to DNA.

In principle, a Hill coefficient close to one indicates that only one γ-s-ATP-activated subunit in the oligomer is required for DNA binding or that the binding of DNA is progressively increased with the number of subunits that are bound to γ-s-ATP. To overcome this argument, we performed an experiment similar to the CE assay described above. The complex of gp16-DNA was assembled in the presence of saturating conditions of γ-s-ATP. After the complex formed, increasing amounts of ADP were added in order to compete with γ-s-ATP for the active sites of gp16 and to ultimately promote the release of DNA. The results exhibited a remarkably cooperative behavior (Fig. 5E,F). From the fractional inhibition plot we extrapolated a Hill coefficient close to 6, indicating that 6 molecules of ADP must be bound to gp16 before dsDNA can be released from the protein. This indicates that only one ATP bound subunit is able to stably bind DNA and prevent ADP mediated release. Furthermore, our results indicate that gp16 most likely binds to dsDNA at only one subunit per round of ATP hydrolysis. As mentioned above, a Hill coefficient close to one indicates that binding of DNA is progressively increased with the number of subunits that are bound to γ-s-ATP. However, the 3.6-nm diameter of the motor channel, as measured from the crystal structure (Guasch, Pous et al., 2002;Badasso, Leiman et al., 2000), suggests that only one dsDNA can be bound within the channel; indicating that dsDNA shifts to a subsequent gp16 subunit upon release of the former. In combination

with the finding that one Walker B mutant gp16 was found to be sufficient to block the motor for DNA packaging, these results support the model that the motor ATPase works sequentially, and upon ATP hydrolysis the subunit of the ATPase gp16 assumes a new conformation and pushes dsDNA away from the subunit and transfers it to an adjacent subunit (Fig. 7).

Mixed oligomer between wildtype and mutants display negative cooperativity and communication between the subunits of gp16 oligomer

The fact that dsDNA only binds to one gp16 subunit at a time suggests that gp16 undergoes cooperativity during translocation. To verify this hypothesis we analyzed ATPase activity by studying the effect on the oligomerization of gp16 when mutant subunits were introduced (Trottier & Guo, 1997;Chen, Trottier et al., 1997). If we assume communication between the subunits of the ATPase, the effect on the ATPase activity mediated by one inactive subunit should be higher than the simple sum of the ATPase activity of the single subunit. When the ATPase activity was measured in the absence of dsDNA, increasing amounts of Walker B mutants added to the overall oligomer of gp16 failed to provide any significant effect on the rate of hydrolysis (Fig. 6A,C), suggesting that each subunit of gp16 is able to hydrolyze ATP independently. On the contrary, when saturating amounts of dsDNA were added to the reaction, we observed a strong negative cooperative effect with a profile that mostly overlapped with the one predicted for the case in which one single inactive subunit is able to inactivate a whole oligomer (Fig. 6B,D); a predicted case calculated from a binomial distribution inhibition assay (Trottier & Guo, 1997;Chen, Trottier et al., 1997). The results suggest that in the presence of dsDNA, a rearrangement occurs within the subunits of gp16 that enables them to communicate between each other and "sense" the nucleotide state of the reciprocal subunit. The fact that dsDNA needs to be present in the reaction indicates that dsDNA binds to the inactive subunit during the catalytic cycle and remains bound to it, which generates a stalled ATP hydrolysis cycle. This observation supports the idea

that only the subunit that is binding to the substrate at any given time is the one that is permitted to hydrolyze ATP, thus performing translocation while the other subunits are in a type of 'stalled' or 'loaded' state. The scenario suggests an extremely high level of coordination on the function of the protein, which is likely the most efficient process to couple energy production with DNA translocation *via* ATP hydrolysis. An effective mechanism of coordination is apparent between gp16 and dsDNA using the hydrolysis cycle as means for regulation.

Direct observation of multiple ATPase gp16s lining up in queue along dsDNA as the initiation step in DNA packaging

The standard notion derived from extensive investigation of viral packaging motors is that the ATPase binds to the procapsid to form a procapsid/ATPase complex as the first step of motor action in DNA packaging (Fujisawa, Shibata et al., 1991;Guo, Peterson et al., 1987a). To investigate the sequence of interaction between motor components during DNA packaging, a fluorescent Cy3-conjugated gp16 was used to visualize the protein. Interestingly, we found that the first step in DNA packaging was the binding of multiple gp16 queued along the dsDNA, as observed by single molecule imaging (Fig. 8 Part I) and by binding affinity studies. Moreover, negatively stained electron microscopy images have been taken of a multimeric gp16 complex along long genomic DNA (Fig. 8 Part II), lending further support to our conclusions.

DNA tightropes were constructed (Kad, Wang et al., 2010), which not only generated a straight DNA chain, but also lifted the DNA a few microns away from the surface of the slide within the sample chamber. Background fluorescence from non-specific binding of Cy3-gp16 to the surface of the slide was therefore eliminated when the focus of the imaging plane was at the Cy3-gp16 molecules on the DNA chains. A string of multiple Cy3 spots representing Cy3-gp16 complexes were bound along the DNA chains (Fig. 8 Part I A-C, E, F). In the absence of DNA, a Cy3 signal was not observed

between the polylysine beads (Fig. 8 Part I D), indicating that the queued Cy3 signals were truly from the multiple Cy3-gp16 bound to the DNA chains. The results suggest that ATPase gp16 lines up in a queue along dsDNA as the initiation step in DNA packaging. This data is in accordance with another study whose results showed that when complexes of procapsid containing partially packaged dsDNA were isolated by sucrose sedimentation, conversion of the complexes to complete the DNA packaging process required ATPase gp16, but not pRNA (Shu & Guo, 2003b). The same publication also indicated that multiple gp16, but only a single hexameric pRNA, was required for packaging (Shu & Guo, 2003b).

It has been previously reported that the terminases of viral DNA packaging motors bind to procapsids, although with an extremely low affinity and efficiency (Shibata, Fujisawa et al., 1987;Morita, Tasaka et al., 1995b;Morita, Tasaka et al., 1995a;Guo, Peterson et al., 1987a;Fujisawa, Shibata et al., 1991;Lee & Guo, 2006). Our finding that gp16 binds to dsDNA first and then moves along dsDNA before reaching and binding to the procapsid is not contradictory to previous findings, rather a further refinement of the previous understanding. We hypothesize that gp16 contains two domains, one for dsDNA binding and one for connector/procapsid binding. In the absence of genomic DNA, gp16 will bind to procapsid, albeit at a lower affinity. The key to understanding the sequence of interaction is based on the relative affinity of the protein for its substrate. Gp16 has a higher binding affinity for genomic DNA compared to that of the procapsid (Fig.9). In the absence of dsDNA, gp16 and other terminases bind to the procapsid (Guo, Peterson et al., 1987a). However, in the presence of genomic DNA, gp16 and other terminases prefer to bind to genomic DNA and track along it until reaching their final destination, the components of the procapsid, and translocated.

To confirm this hypothesis, we further investigated the interaction of ATPase gp16 with the procapsid (Fig. 9). We discovered that gp16 had the tendency to bind to all kinds of substrate, including nonspecifically to the procapsid. No significant difference was observed during the formation of the

procapsid/gp16 complex in the presence or absence of pRNA (Fig. 9), which has been reported to serve as the bridge for gp16 binding to procapsid (Lee & Guo, 2006). The estimated dissociation constant was calculated and gp16 was found to have a 10-fold higher affinity for dsDNA than for the prohead/pRNA complex. Although the ATPase is hypothesized to contain both dsDNA and procapsid binding domains, it is suggested that the ATPase prefers to bind to the procapsid only after tracking along the genomic DNA; that is, gp16 prefers to bind to genomic DNA first before reaching the procapsid.

Direct observation of ATP-dependent motion of gp16 along dsDNA in real-time by single molecule fluorescence imaging

The motion of gp16 along the lifted dsDNA tightrope was observed by single molecule fluorescence imaging. Sequential images were taken after washing with different buffers to illustrate the displacement of Cy3-gp16 over time. When the sample was washed with a buffer, a total of 195 Cy3-gp16 spots were studied. In the absence of ATP, the vast majority of these Cy3-gp16 spots did not show any motion along the DNA chain. After 20 mM ATP was added to the washing buffer, active motion of eGFP-gp16 along the dsDNA was observed, as shown by the sequential images (Fig. 8 Part I G) and kymographs (Fig. 8 Part I H). Actual motion videos can be found at http://nanobio.uky.edu/movie.html using Internet Explorer.

Translocation of dsDNA helix by revolution without involvement of coiling or tension force

It has previously been demonstrated that the connector is a one way valve (Schwartz, Fang et al., 2012;Fang, Jing et al., 2012;Jing, Haque et al., 2010) that only allows dsDNA to move into the procapsid, but does not allow movement in the opposite direction. Gp16, which is bridged by pRNA to associate with the connector, is expected to be the pushing force (Fig. 10A). The binding of ATP to

one subunit stimulates gp16 to adapt a conformation with high affinity for dsDNA, while ATP hydrolysis forces gp16 to assume a new conformation with lower affinity for dsDNA, thus pushing dsDNA away from the subunit and transferring it to an adjacent subunit (Fig. 10). Since the contact of the connector with dsDNA chain is transferred from one point on the phosphate backbone to another, rotation of the hexameric ring or the dsDNA is not required. One ATP is hydrolyzed in each transitional step, and six ATPs are consumed for one cycle to translocate dsDNA one helical turn of 360° (10.5 base pairs). The binding of gp16 to the same phosphate backbone chain, but at a location 60° different from the last subunit, urges dsDNA to move forward 1.75 base pairs (10.5 bp per turn ÷ 6 ATP = 1.75 bp/ATP), agreeing with the 2 bp/ATP(Guo, Peterson et al., 1987b) or 1.8 bp/ATP previously quantified empirically(Morita, Tasaka et al., 1993).

Translocation of dsDNA helix by revolution through the 30°-tilted connector subunits facilitated by anti-parallel displacement between dsDNA helix and the connector portal protein

Extensive research has also been undertaken to understand the role of the connector during packaging, especially after the crystal structure of the connector had been elucidated. An interesting phenomenon was observed. All 12 subunits of the connector protein tilt at a 30° angle, in a configuration anti-parallel to the dsDNA helix during packaging, to form the channel (Guasch, Pous et al., 2002;Badasso, Leiman et al., 2000). The anti-parallel arrangement can be visualized from an external viewpoint in which dsDNA propels through the connector potentially making contact at every 30° subunit (Fig. 11). This anti-parallel arrangement tends to argue against the bolt and nut mechanism. This structural arrangement greatly facilitates controlled motion, supporting the conclusion that dsDNA revolves through the connector channel without producing a coiling or torsion force, and touching each of the 12 connector subunits in 12 discrete steps of 30° transitions for each helical pitch (360° ÷ 12 = 30°) (Fig. 11D). Moreover, the 30° angle of each connector subunit coincides nicely with the crystal

structure of the spiral cellular clamp loader and the grooves of dsDNA (Mayanagi, Kiyonari et al., 2009;McNally, Bowman et al., 2010). Nature has created and evolved a clever rotating machine to reduce the torque force and to translocate the DNA double helix which actually avoids the difficulties associated with rotation such as DNA supercoiling seen in many other processes.

DISCUSSION

A rotation mechanism of viral DNA packaging motor has long been proposed (Hendrix, 1978) and is well-liked by the scientific community. However, studies combining the methods of single-molecule force spectroscopy with polarization-sensitive single-molecule fluorescence trap (Hugel, Michaelis et al., 2007) have suggested that the connector does not rotate. The suggestion of non-rotation by the connector was further supported by the experiment in which the connector was covalently linked to the capsid protein of the procapsid (Baumann, Mullaney et al., 2006;Maluf & Feiss, 2006). When the connector and the procapsid protein were fused to each other, rotation of the connector within the procapsid was not possible. However, the motors were still active in packaging, implying that connector rotation is not necessary for DNA packaging. Furthermore, since the connector does not rotate, there is no reason to believe that gp16 will rotate since the gp16 ring is tightly bound to the pRNA ring (Lee & Guo, 2006) that is immobilized to the external end of the stationary connector. The finding that phi29 DNA packaging motor utilizes a revolution instead of rotation mechanism is in a good agreement with all data reported in the history. Since the revolution mechanism is independent of stoichiometry and motors with different oligomeric ATPase subunits all can execute the revolution mechanism the discovery of the revolution mechanism might reconcile the stoichiometry discrepancy among many phage systems for which the ATPase was found to be present as tetramer{Maluf, 2006 5467 /id}, hexamer (Guo, Zhang et al., 1998;Zhang, Lemieux et al., 1998;Hendrix, 1998;Shu, Zhang et

al., 2007;Xiao, Zhang et al., 2008;Moll & Guo, 2007;Shu, Zhang et al., 2007;Xiao, Demeler et al., 2010;Zhang, Endrizzi et al., 2012), and nonamers (Roy, Bhardwaj et al., 2011).

The connector was recently revealed to only allow for unidirectional movement of dsDNA (Jing, Haque et al., 2010), and a model using a "push through a one-way valve" mechanism was described (Schwartz, Fang et al., 2012;Fang, Jing et al., 2012) which is in accordance with the previously proposed ratchet (Serwer, 2003) and compression (Ray, Sabanayagam et al., 2010;Ray, Ma et al., 2010) models. This mechanism describes dsDNA being pushed by the ATPase gp16 through the connector which functions as a valve to prevent DNA from reversing out of the capsid during the packaging process (Black, 1989;Feiss & Rao, 2012;Casjens, 2011;Guo & Lee, 2007). The finding of a revolution hexamer mechanism is seemingly contradictory to the publications reporting the existence of four bursts of translocation per helical turn of genomic B-type dsDNA (Moffitt, Chemla et al., 2009;Yu, Moffitt et al., 2010). Although there was much discrepancy in step size and pulse, the data for the four step pause looks quite strong. To address the inconsistencies, we investigated the mechanism of the generation of the four pause steps and found that the four steps of pauses were caused by the dsDNA revolving through the four lysine rings (Zhao, Khisamutdinov et al., 2013) (conditionally accepted). Connector crystal analysis (Guasch, Pous et al., 2002;Badasso, Leiman et al., 2000) has revealed that the dominantly negatively charged phi29 connector interior channel surface is decorated with 48 positively charged lysine residues existing as four 12-lysine rings derived from the 12 protein subunits that enclose the channel. It has been proposed that these electropositive lysine residues interact with the electronegative phosphate backbone of DNA during DNA translocation through the channel (Guasch, Pous et al., 2002;Badasso, Leiman et al., 2000). Although the lysine residues were not found to be essential for DNA entry(Fang, Jing et al., 2012;Zhang, Schwartz et al., 2012), the four positively

charged residues have been shown to influence more or less the DNA translocation speed (Fang, Jing et al., 2012;Grimes, Ma et al., 2011;Geng, Huaming et al., 2013).

Based on the crystal structure (Guasch, Pous et al., 2002;Badasso, Leiman et al., 2000), the length of the connector channel is ~7 nm. The interior of the channel is negatively charged and four lysine rings (K200, K209, K234, and K235) are scattered as four rings inside the channel. Vertically, these four lysine layers fall within a 3.7 nm (Guasch, Pous et al., 2002;Badasso, Leiman et al., 2000) range and are spaced approximately ~0.9 nm apart ((~3.7 nm)⁄4=~0.9 nm). Since lysine residues K234 and K235 lie in the inner loop of the connector between residues 229 to 246, of which the residues were missing in the crystal structure, the two residues close to the boundary of the inner loops were used to estimate their location. Since B-type dsDNA has a pitch of 0.34 nm per base pair as a rise along its axis, 0.9 nm ÷ 0.34 nm.bp^{-1} = ~2.6 bp per rise. This value agrees with the aforementioned finding that DNA packages in four 2.5 bp steps for each helical turn (Moffitt, Chemla et al., 2009;Yu, Moffitt et al., 2010). We suggest that the four distinct, alternating positively and negatively charged property of the channel wall alters the speed of DNA translocation and results in four steps of pause during revolution advancement (Zhao, Khisamutdinov et al., 2013). Thus the revolution mechanism is not contradictory to the finding of four steps of pause. However, the authors interpreted their solid findings of pauses as five motor subunits with one subunit inactive resulting in four steps of burst, a model that is seemly novel but does not exist.

Acknowledgements

We would like to thank Dr. Guo-Min Li for his valuable comments, Zhengyi Zhao, Emil Khisamutdinov, and Hui Li for their diligent work on the animation figures, Drs. Bruce Maley and Mary Gail Engle for EM images, and Jeannie Haak for editing this manuscript. The work was

supported by NIH grants R01 EB003730, R01 EB012135, and U01 CA151648 to PG, who is a co-founder of Kylin Therapeutics, Inc, and Biomotor and Nucleic Acids Nanotech Development, Ltd.

FIGURE LEGENDS

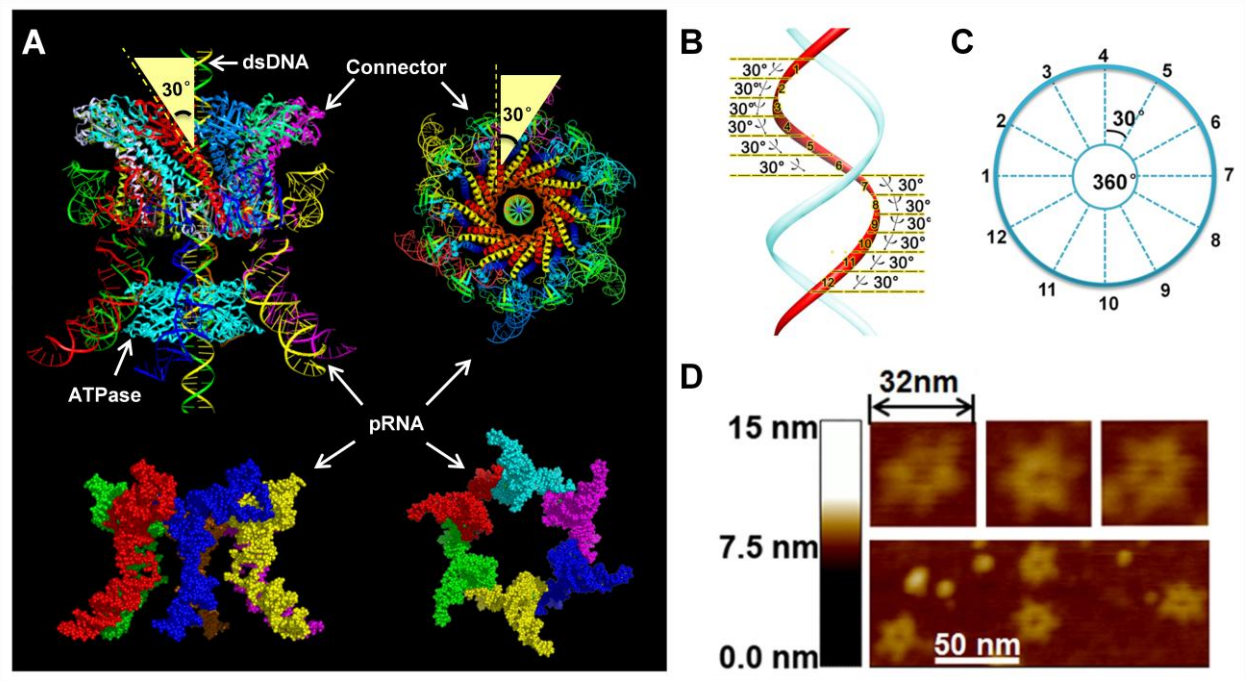

Figure 1. Depiction of structure and function of phi29 DNA-packaging motor. (A) Model of hexameric pRNA based on crystal structure and the 30° tilting of the channel subunits of the connector; (B) DsDNA showing the change of 30° angle between two adjacent connector subunits; (C) Connector showing the change of 30° angle between two adjacent connector subunits; (D) AFM images of the hexameric pRNA with 7-nt loops.

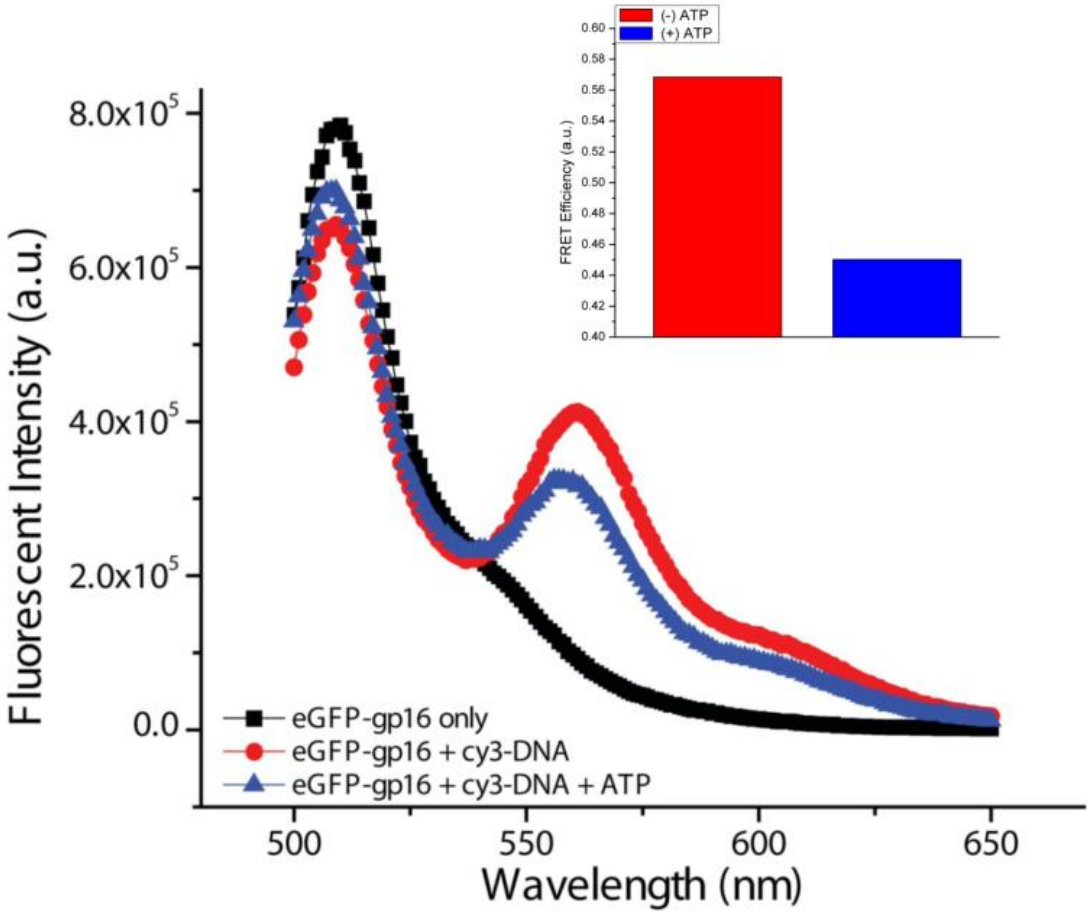

Figure 2. FRET Assay of fluorogenic ATPase and short dsDNA. eGFP-gp16 was incubated with Cy3-DNA and with (blue line) and without ATP (red line) and excited at 480 nm. Energy transfer occurs between the two fluorophores indicating the gp16 and DNA are in close proximity.

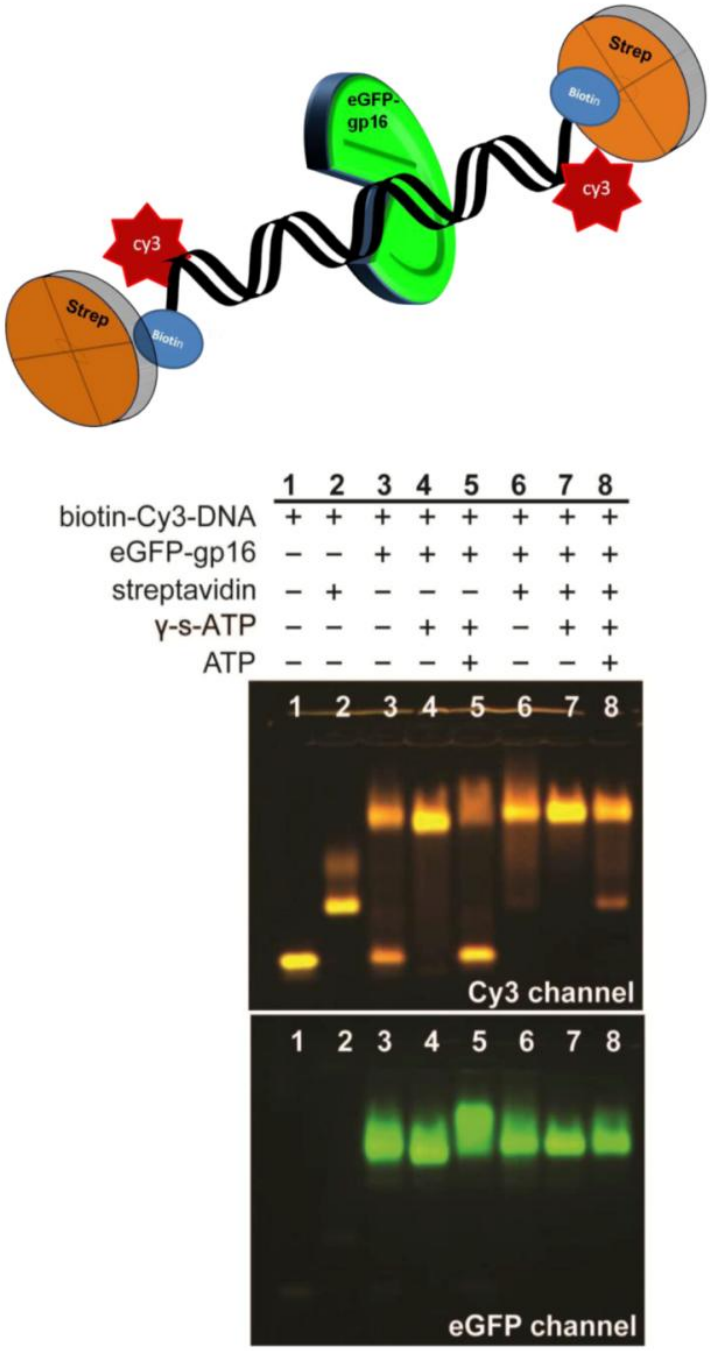

Figure 3. Differentiation of gp16 walking along or dissociating from dsDNA by EMSA using terminally-hindered short dsDNA with two biotin at both ends. Fluorogenic Cy3-dsDNA was incubated with GFP-gp16, non-hydrolyzable γ-S-ATP and streptavidin in different combinations. The complexes were then electrophoresed through an agarose gel and scanned for Cy3 fluorescence of DNA and GFP fluorescence of gp16.

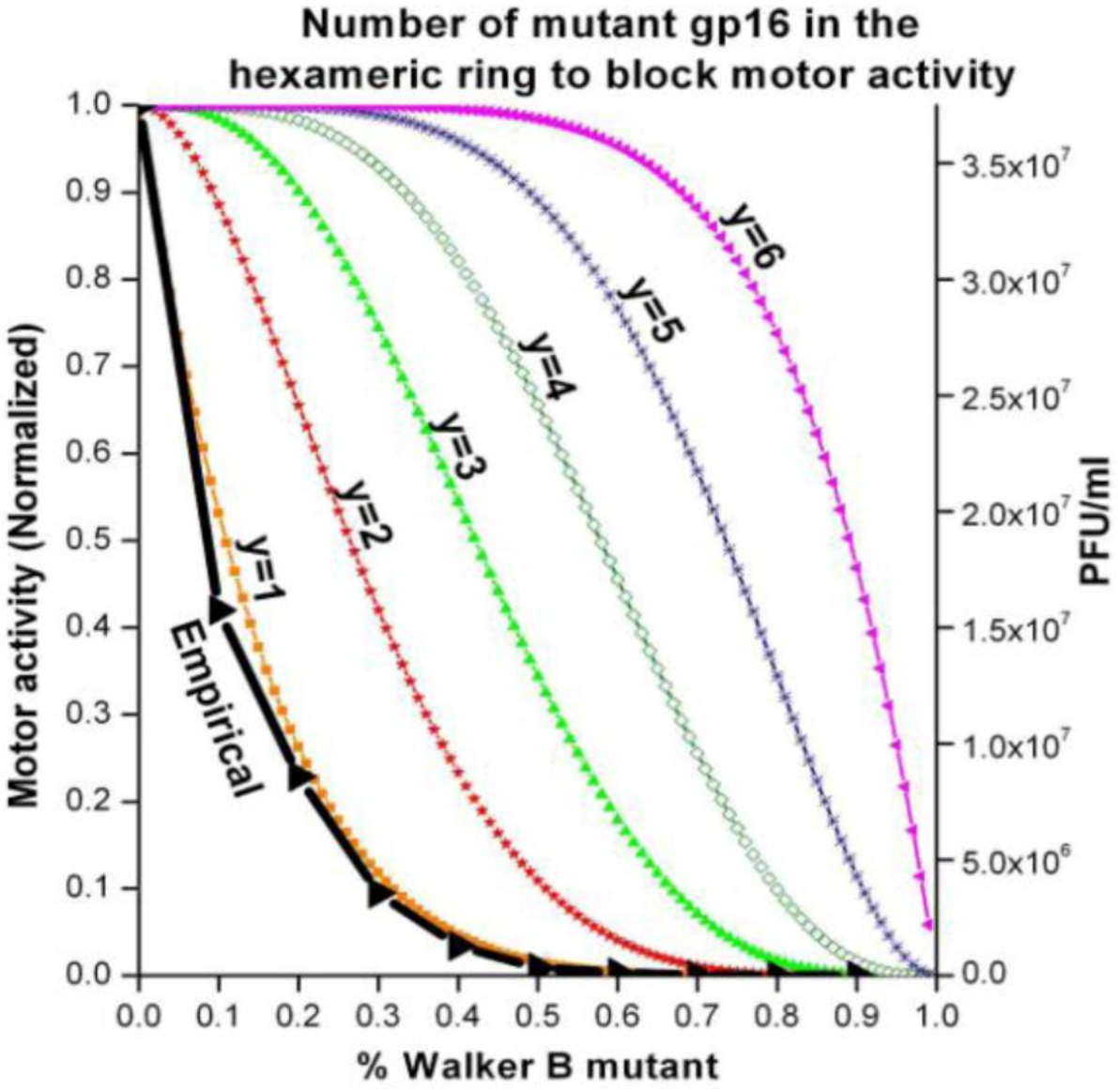

Figure 4. Binomial distribution assay to determine the minimum number (y) of Walker B mutant eGFP-gp16 in the hexameric ring to block the motor activity. The equation$(p+q)^6 = \binom{6}{0}p^6 + \binom{6}{1}p^5q^1 + \binom{6}{2}p^4q^2 + \binom{6}{3}p^3q^3 + \binom{6}{4}p^2q^4 + \binom{6}{5}p^1q^5 + \binom{6}{6}q^6$ is used, where p and q represent the ratio of wild type and mutant eGFP-gp16 respectively, and p+q=1. If y=1, then the motor activity will be $\binom{6}{0}p^6$; if y=2, then the motor activity will be $\binom{6}{0}p^6 + \binom{6}{1}p^5q^1$; if y=3, then the motor activity will be $\binom{6}{0}p^6 + \binom{6}{1}p^5q^1 + \binom{6}{2}p^4q^2$; if y=4, then the motor activity will be $\binom{6}{0}p^6 + \binom{6}{1}p^5q^1 + \binom{6}{2}p^4q^2 + \binom{6}{3}p^3q^3$; if y=5, then the motor activity will be $\binom{6}{0}p^6 + \binom{6}{1}p^5q^1 + \binom{6}{2}p^4q^2 + \binom{6}{3}p^3q^3 + \binom{6}{4}p^2q^4$; if y=6, then the motor activity will be $\binom{6}{0}p^6 + \binom{6}{1}p^5q^1 + \binom{6}{2}p^4q^2 + \binom{6}{3}p^3q^3 + \binom{6}{4}p^2q^4 + \binom{6}{5}p^1q^5$.

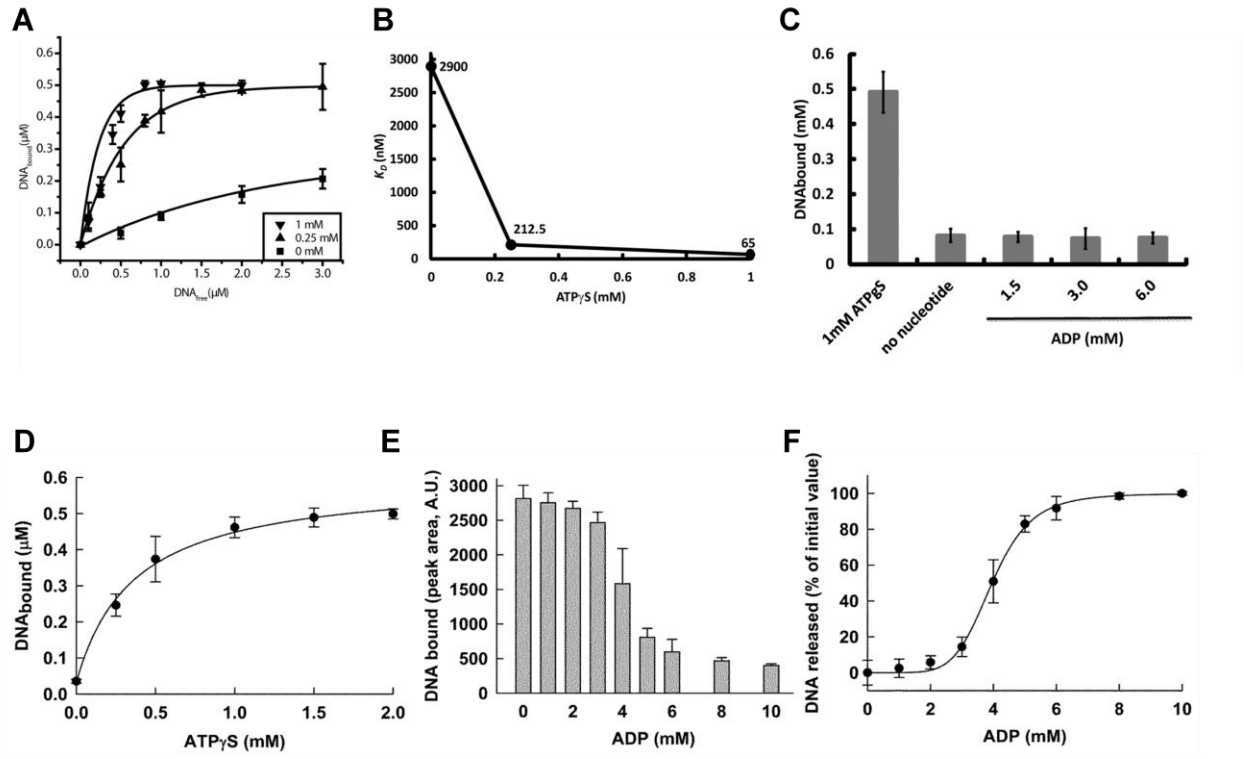

Figure 5. Data demonstrating only one γ-s-ATP is sufficient to bind to one subunit of the hexameric gp16 complex and promote a high affinity state for dsDNA. Sequential binding of gp16 for dsDNA substrate involves γ-s-ATP substep. (A) The K_d for dsDNA in the presence (triangles) and absence (squares) of γ-s-ATP. (B) The relative K_d of gp16 decreased 40-fold as the concentration of γ-s-ATP increased from 0 mM to 1 mM. (C) ADP, a derivative of ATP hydrolysis, was unable to promote binding and had the similar effect as no nucleotide addition. The hyperbolic curve (D) suggests a cooperativity factor of 1, indicating that one γ-s-ATP is sufficient to produce the high affinity state of gp16 for DNA. DNA releases from the complex DNA-gp16-γ-s-ATP mediated by ADP (E), forming a sigmoidal curve (F) with a cooperativity factor of 6 indicating that all 6 subunits of gp16 need to be bound to ADP to release DNA from the protein.

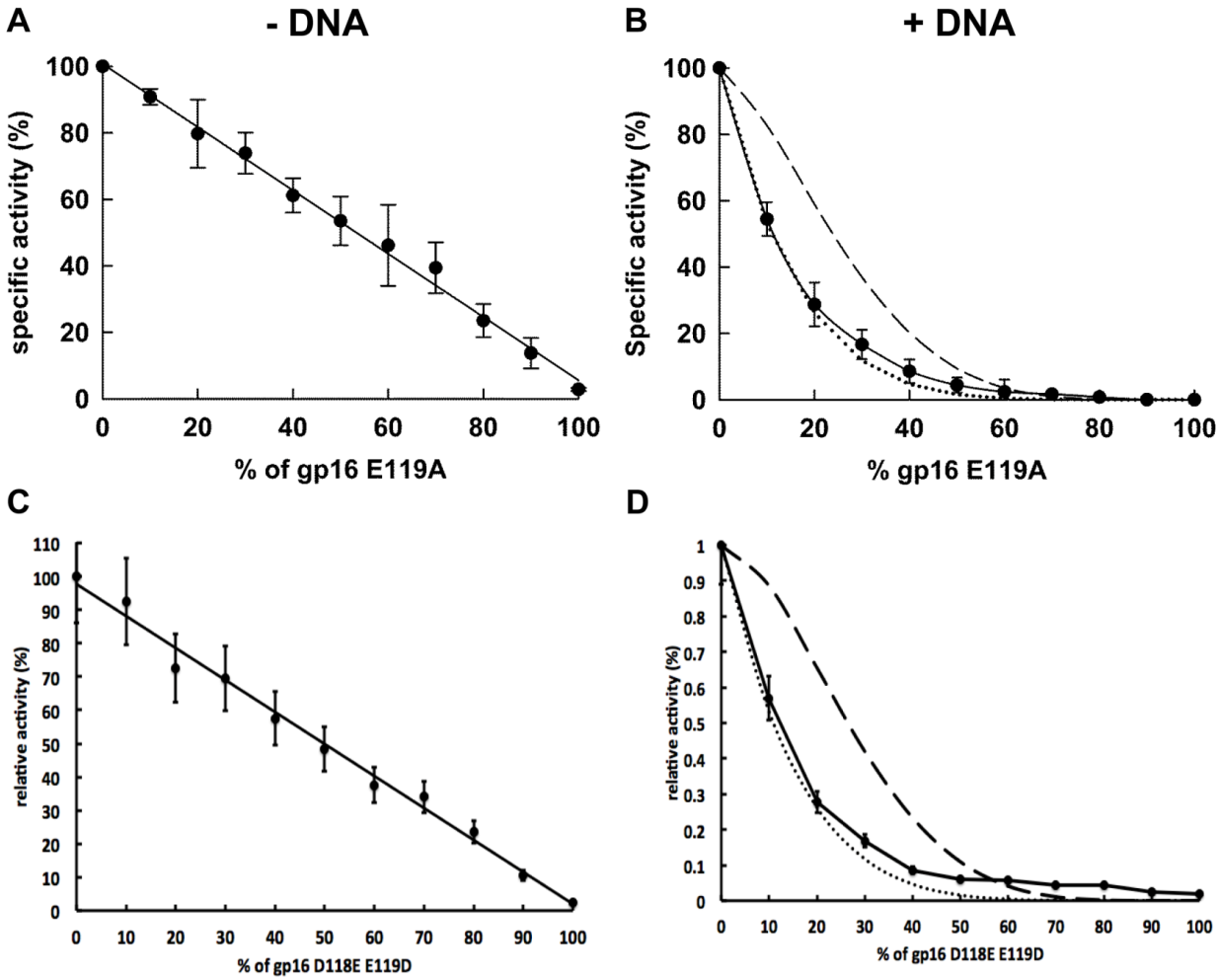

Figure 6. ATPase inhibition assay of Walker B mutants reveal complete negative cooperativity. The inhibition ability of the Walker B mutants E119A and D118E/E119D was assayed by ATPase activity to determine the theoretical model in the absence (left) and presence (right) of dsDNA. In the presence of DNA (right), the experimental data (solid line) overlapped with the theoretical curve indicating that one inactive subunits (dotted line) within the hexamer are able to completely block the activity of the hexameric gp16 and abolish gp16's ability to hydrolyze ATP, demonstrating negative cooperativity. The dashed line is the theoretical curve representing two inactive subunits are necessary for complete inhibition of the hexamer.

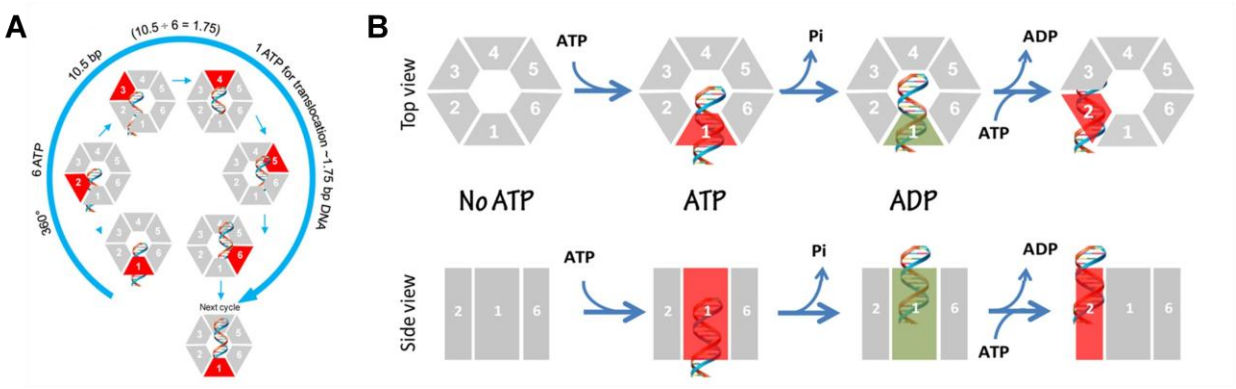

Figure 7. Schematic of gp16 binding to DNA and mechanism of sequential revolution in translocating genomic DNA. The connector is a one way valve that allows dsDNA to move into the procapsid, but does not allow movement in the opposite direction. Gp16, which is bridged by pRNA to associate with the connector, is the pushing force. The binding of ATP to one subunit stimulates gp16 to adapt to a conformation with a higher affinity for dsDNA. ATP hydrolysis forces gp16 to assume a new conformation with a lower affinity for dsDNA, thus pushing dsDNA away from the subunit and transferring it to an adjacent subunit. DsDNA moves forward 1.75 base pairs when gp16 binds at a location 60^{o} different from last subunit on the same phosphate backbone chain. Rotation of the hexameric ring or the dsDNA is not required since the dsDNA chain is transferred from one point on the phosphate backbone to another. In each transitional step, one ATP is hydrolyzed, and in one cycle, six ATPs are required to translocate dsDNA one helical turn of 360^{o} (10.5 base pairs). Please see the website http://nanobio.uky.edu/movie.html using Internet Explorer for animations.

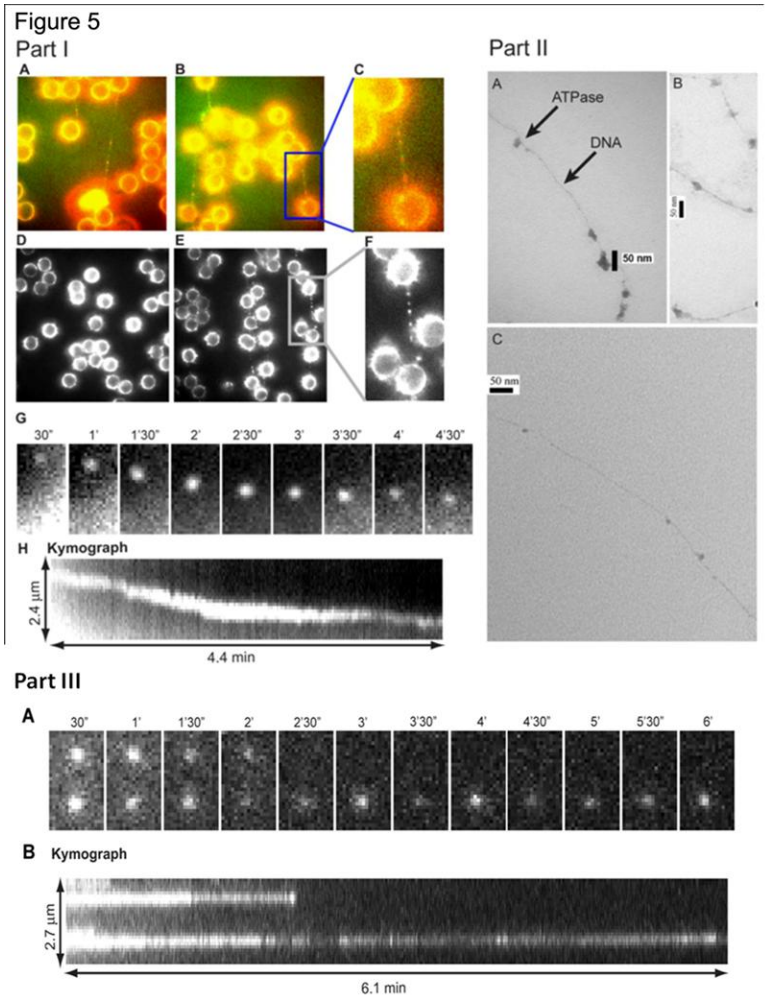

Figure 8. Part I. Direct observation of ATPase complex queued and moving along dsDNA. Cy3 conjugated gp16 was incubated with (A, B, E) and without (D) phi29 genomic dsDNA, tethered between two polylysine beads where (C, F) are magnified images of the framed regions of (B, E), respectively. (A-C) are overlapped pseudocolor images indicating the binding of Cy3-labeled gp16 along the To-Pro-3 stained dsDNA chain (Red: Cy3-gp16; Green: To-Pro-3 DNA). (G, H) The motion of the Cy3-gp16 spot was analyzed and a kymograph was produced to characterize the ATPase walking. (Use Internet Explorer to view website http://nanobio.uky.edu/movie.html for actual motion videos). **Part II. Negatively-stained transmission electron microscopy images of ATPase queued along dsDNA.** gp16 was bound to non-specific dsDNA in queue. **Part III. Recording of two Cy3-gp16/dsDNA complexes showing motionless gp16 spots in a buffer containing no ATP.** (A) Sequential images of the recording. (B) Kymograph of the two spots.

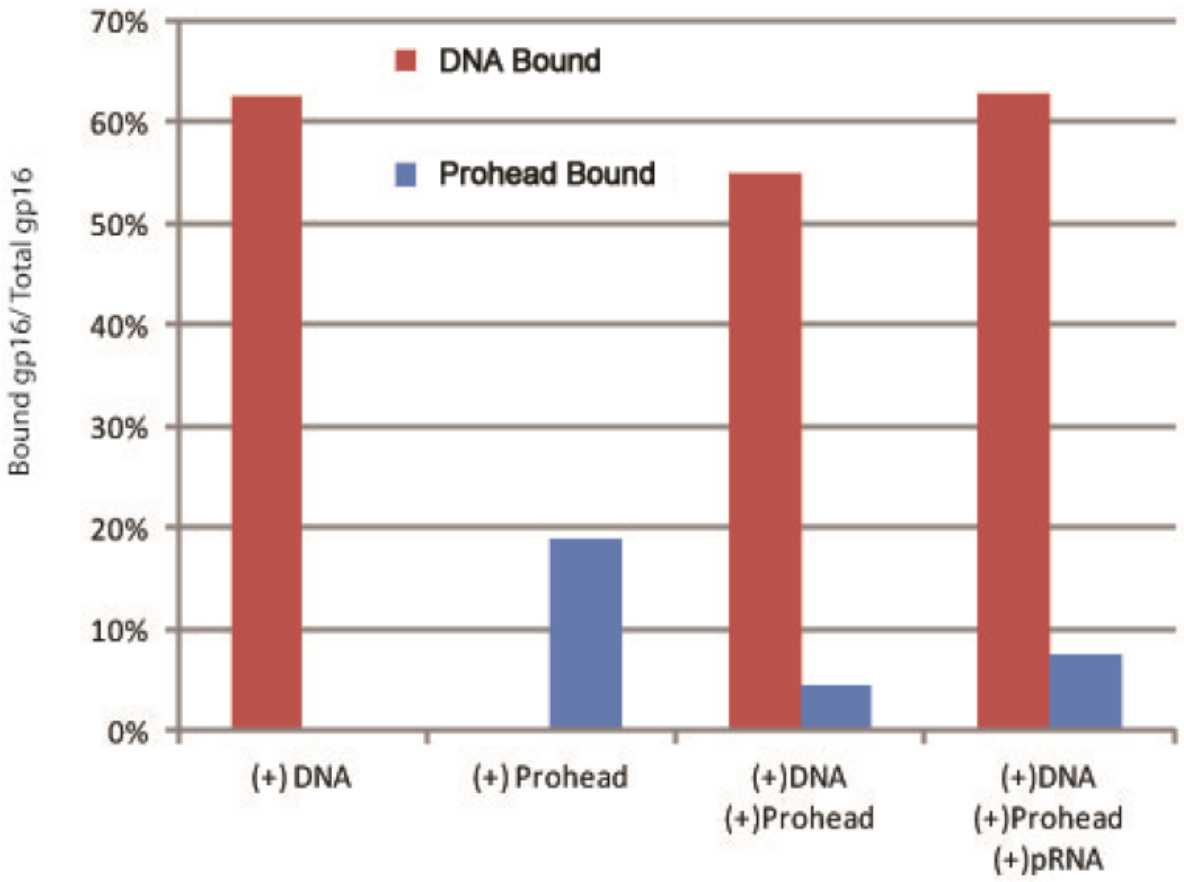

Figure 9. Comparison of binding affinity of gp16 to dsDNA and procapsid/pRNA complex using sucrose sedimentation. Ratio of prohead-bound and DNA-bound gp16 under different treatments where the percent of bound gp16 to total gp16 is expressed, showing gp16's affinity to DNA is much greater than to prohead/pRNA complex.

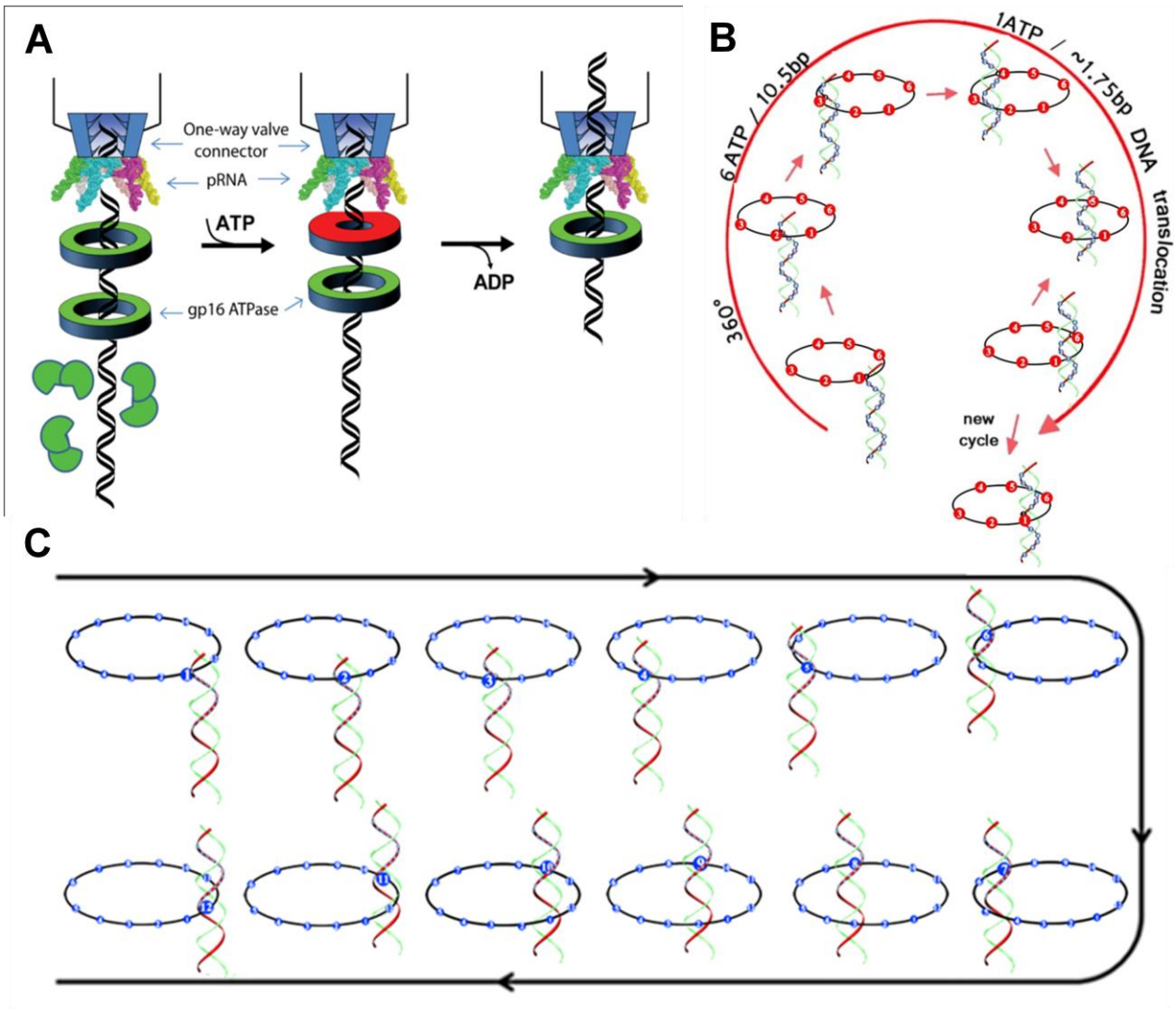

Figure 10. Mechanism of sequential revolution in translocating genomic DNA. Connector is a one way valve (Lee & Guo, 1994;Hendrix, 1978;Hugel, Michaelis et al., 2007) that allows dsDNA to move into the procapsid but does not allow movement in the opposite direction. Binding of ATP to one gp16 subunit stimulates it to adapt a conformation with higher affinity for dsDNA. ATP hydrolysis forces gp16 to assume a new conformation with lower affinity for dsDNA, thus pushing dsDNA away from this subunit and transferring it to an adjacent subunit. Binding of gp16 to the same phosphate backbone chain but at a location 60° different from last subunit urges dsDNA to move forward 1.75 base pairs. Since the dsDNA chain is transferred from one point on the phosphate backbone to another point, the rotation of the hexameric ring or the dsDNA is not required. (C) The revolution of dsDNA along the 12 subunits of the connector channel.

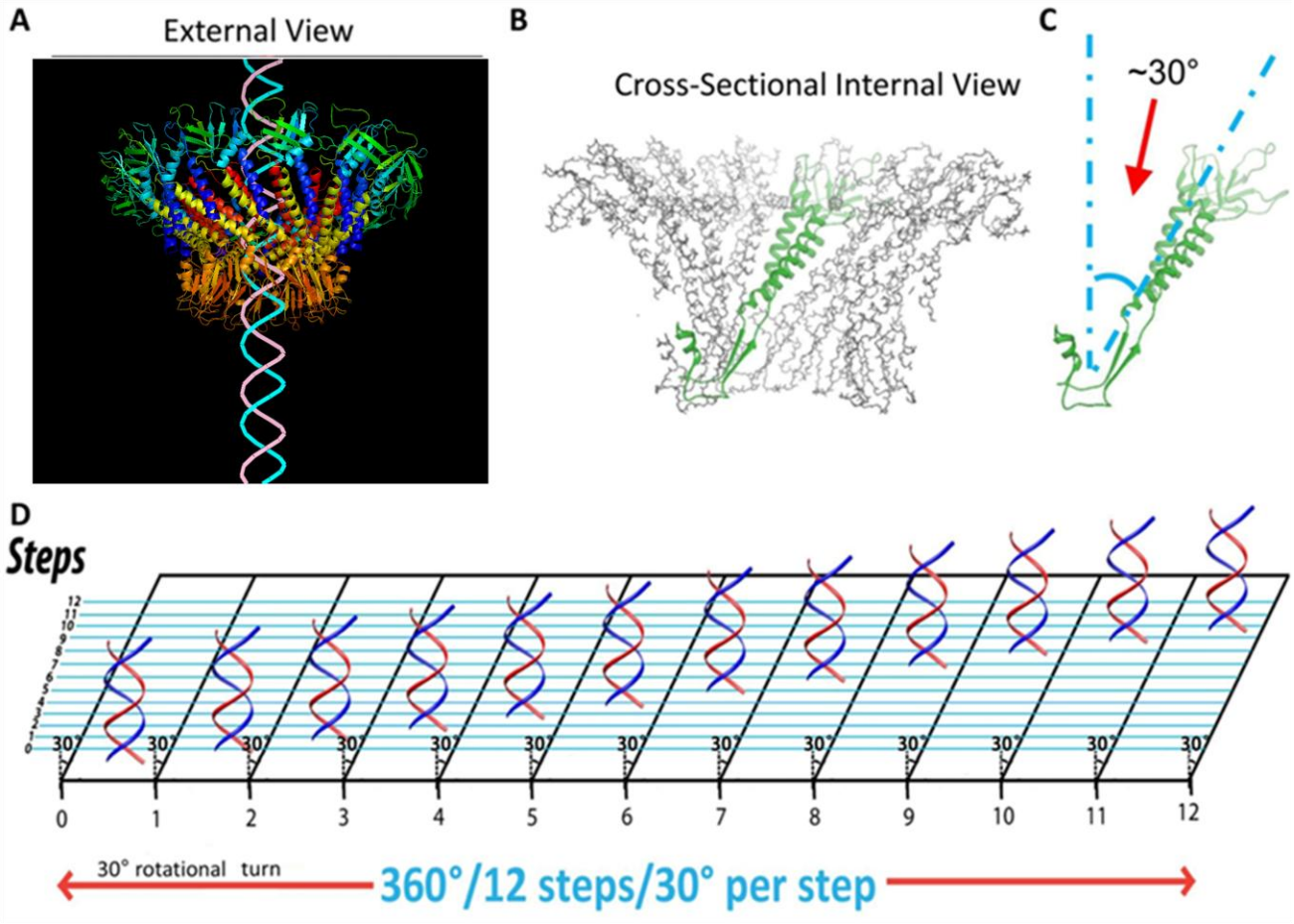

Figure 11. **DNA revolves and transports through 30° tilted connector subunits facilitated by anti-parallel helices between dsDNA helix and connector protein subunits.** The anti-parallel configuration can be visualized in an external view (A) in which DNA revolves through the connector making contacts at every 30° subunit (B,C). A planar view is suggested (D) in which DNA is advanced and travels along the circular wall of the connector channel with no torsion or coiling force through the connector channel touching each subunit translating to 12 discrete steps of 30° revolving turns for each step.

Reference List

Aathavan, K., Politzer, A. T., Kaplan, A., Moffitt, J. R., Chemla, Y. R., Grimes, S., Jardine, P. J., Anderson, D. L., Bustamante, C., 2009. Substrate interactions and promiscuity in a viral DNA packaging motor. Nature 461, 669-673.

Amitani, I., Baskin, R. J., Kowalczykowski, S. C., 2006. Visualization of Rad54, a chromatin remodeling protein, translocating on single DNA molecules. Mol.Cell 23, 143-148.

Ammelburg, M., Frickey, T., Lupas, A. N., 2006. Classification of AAA+ proteins. Journal of Structural Biology 156, 2-11.

Badasso, M. O., Leiman, P. G., Tao, Y., He, Y., Ohlendorf, D. H., Rossmann, M. G., Anderson, D., 2000. Purification, crystallization and initial X-ray analysis of the head- tail connector of bacteriophage phi29. Acta Crystallogr D Biol Crystallogr 56 (Pt 9), 1187-1190.

Bath, J., Wu, L. J., Errington, J., Wang, J. C., 2000. Role of Bacillus subtilis SpoIIIE in DNA transport across the mother cell-prespore division septum. Science 290, 995-997.

Baumann, R. G., Mullaney, J., Black, L. W., 2006. Portal fusion protein constraints on function in DNA packaging of bacteriophage T4. Mol Microbiol. 61, 16-32.

Black, L. W., 1989. DNA Packaging in dsDNA bacteriophages. Annual Review of Microbiology 43, 267-292.

Casjens, S. R., 2011. The DNA-packaging nanomotor of tailed bacteriophages. Nat Rev.Microbiol. 9, 647-657.

Chemla, Y. R., Aathavan, K., Michaelis, J., Grimes, S., Jardine, P. J., Anderson, D. L., Bustamante, C., 2005. Mechanism of force generation of a viral DNA packaging motor. Cell. 122, 683-692.

Chen, C., Guo, P., 1997. Sequential action of six virus-encoded DNA-packaging RNAs during phage phi29 genomic DNA translocation. Journal of Virology 71, 3864-3871.

Chen, C., Trottier, M., Guo, P., 1997. New approaches to stoichiometry determination and mechanism investigation on RNA involved in intermediate reactions. Nucleic Acids Symposium Series 36, 190-193.

Chen, Y. J., Yu, X., Egelman, E. H., 2002. The hexameric ring structure of the Escherichia coli RuvB branch migration protein. J.Mol.Biol. 319, 587-591.

Chistol, G., Liu, S., Hetherington, C. L., Moffitt, J. R., Grimes, S., Jardine, P. J., Bustamante, C., 2012. High Degree of Coordination and Division of Labor among Subunits in a Homomeric Ring ATPase. Cell 151, 1017-1028.

Demarre, G., Galli, E., Barre, F. X., 2013. The FtsK Family of DNA Pumps. Adv.Exp.Med.Biol 767, 245-262.

Egelman, H. H., Yu, X., Wild, R., Hingorani, M. M., Patel, S. S., 1995. Bacteriophage T7 helicase/primase proteins form rings around single- stranded DNA that suggest a general structure for hexameric helicases. Proc Natl Acad Sci U.S.A 92, 3869-3873.

Fang, H., Jing, P., Haque, F., Guo, P., 2012. Role of channel Lysines and "Push Through a One-way Valve" Mechanism of Viral DNA packaging Motor. Biophysical Journal 102, 127-135.

Feiss, M., Rao, V. B., 2012. The Bacteriophage DNA Packaging Machine Viral Molecular Machines. In: M. G. Rossmann, V. B. Rao (Eds.), Springer US, pp. 489-509.

Fujisawa, H., Shibata, H., Kato, H., 1991. Analysis of interactions among factors involved in the bacteriophage T3 DNA packaging reaction in a defined *in vitro* system. Virology 185, 788-794.

Geng, J., Huaming, F., shaoying, W., Peixuan, G., 2013. Channel Size Conversion of Phi29 DNA-Packaging Nanomotor for Discrimination of Single- and Double-Stranded DNA and RNA. ACS Nano.

Gomis-Ruth, F. X., Moncalian, G., Perez-Luque, R., Gonzalez, A., Cabezon, E., de la, C. F., Coll, M., 2001. The bacterial conjugation protein TrwB resembles ring helicases and F1- ATPase. Nature 409, 637-641.

Grainge, I., 2008. Sporulation: SpoIIIE is the key to cell differentiation. Curr.Biol. 18, R871-R872.

Grainge, I., Bregu, M., Vazquez, M., Sivanathan, V., Ip, S. C., Sherratt, D. J., 2007. Unlinking chromosome catenanes in vivo by site-specific recombination. EMBO Journal 26, 4228-4238.

Grainge, I., Lesterlin, C., Sherratt, D. J., 2011. Activation of XerCD-dif recombination by the FtsK DNA translocase. Nucleic Acids Research 39, 5140-5148.

Grimes, S., Anderson, D., 1990. RNA Dependence of the Bateriophage phi29 DNA Packaging ATPase. J.Mol.Biol. 215, 559-566.

Grimes, S., Ma, S., Gao, J., Atz, R., Jardine, P. J., 2011. Role of phi29 connector channel loops in late-stage DNA packaging. J.Mol.Biol. 410, 50-59.

Guasch, A., Pous, J., Ibarra, B., Gomis-Ruth, F. X., Valpuesta, J. M., Sousa, N., Carrascosa, J. L., Coll, M., 2002. Detailed architecture of a DNA translocating machine: the high- resolution structure of the bacteriophage phi29 connector particle. J.Mol.Biol. 315, 663-676.

Guenther, B., Onrust, R., Sali, A., O'Donnell, M., Kuriyan, J., 1997. Crystal structure of the delta' subunit of the clamp-loader complex of E. coli DNA polymerase III. Cell 91, 335-345.

Guo, P., Erickson, S., Anderson, D., 1987. A small viral RNA is required for *in vitro* packaging of bacteriophage phi29 DNA. Science 236, 690-694.

Guo, P., Grimes, S., Anderson, D., 1986. A defined system for *in vitro* packaging of DNA-gp3 of the *Bacillus subtilis* bacteriophage phi29. Proc.Natl.Acad.Sci.USA 83, 3505-3509.

Guo, P., Peterson, C., Anderson, D., 1987a. Initiation events in *in vitro* packaging of bacteriophage ϕ29 DNA-gp3. Journal of Molecular Biology 197, 219-228.

Guo, P., Peterson, C., Anderson, D., 1987b. Prohead and DNA-gp3-dependent ATPase activity of the DNA packaging protein gp16 of bacteriophage ϕ29. Journal of Molecular Biology 197, 229-236.

Guo, P., Zhang, C., Chen, C., Trottier, M., Garver, K., 1998. Inter-RNA interaction of phage phi29 pRNA to form a hexameric complex for viral DNA transportation. Molecular Cell 2, 149-155.

Guo, P. X., Lee, T. J., 2007. Viral nanomotors for packaging of dsDNA and dsRNA. Molecular Microbiology 64, 886-903.

Hendrix, R. W., 1998. Bacteriophage DNA packaging: RNA gears in a DNA transport machine (Minireview). Cell 94, 147-150.

Hendrix, R. W., 1978. Symmetry mismatch and DNA packaging in large bacteriophages. Proc.Natl.Acad.Sci.USA 75, 4779-4783.

Huang, L. P., Guo, P., 2003a. Use of acetone to attain highly active and soluble DNA packaging protein gp16 of phi29 for ATPase assay. Virology 312(2), 449-457.

Huang, L. P., Guo, P., 2003b. Use of PEG to acquire highly soluble DNA-packaging enzyme gp16 of bacterial virus phi29 for stoichiometry quantification. J Virol Methods 109, 235-244.

Hugel, T., Michaelis, J., Hetherington, C. L., Jardine, P. J., Grimes, S., Walter, J. M., Faik, W., Anderson, D. L., Bustamante, C., 2007. Experimental test of connector rotation during DNA packaging into bacteriophage phi29 capsids. Plos Biology 5, 558-567.

Hwang, Y., Catalano, C. E., Feiss, M., 1996. Kinetic and mutational dissection of the two ATPase activities of terminase, the DNA packaging enzyme of bacteriophage lambda. Biochemistry 35, 2796-2803.

Ibarra, B., Valpuesta, J. M., Carrascosa, J. L., 2001. Purification and functional characterization of p16, the ATPase of the bacteriophage phi29 packaging machinary. Nucleic Acids Research 29(21), 4264-4273.

Iyer, L. M., Leipe, D. D., Koonin, E. V., Aravind, L., 2004. Evolutionary history and higher order classification of AAA plus ATPases. Journal of Structural Biology 146, 11-31.

Iyer, L. M., Makarova, K. S., Koonin, E. V., Aravind, L., 2004. Comparative genomics of the FtsK-HerA superfamily of pumping ATPases: implications for the origins of chromosome segregation, cell division and viral capsid packaging. Nucleic Acids Research 32, 5260-5279.

Jimenez, J., Santisteban, A., Carazo, J. M., Carrascosa, J. L., 1986. Computer graphic display method for visualizing three-dimensional biological structures. Science 232, 1113-1115.

Jing, P., Haque, F., Shu, D., Montemagno, C., Guo, P., 2010. One-Way Traffic of a Viral Motor Channel for Double-Stranded DNA Translocation. Nano Lett. 10 (9), 3620-3627.

Kad, N. M., Wang, H., Kennedy, G. G., Warshaw, D. M., Van, H. B., 2010. Collaborative dynamic DNA scanning by nucleotide excision repair proteins investigated by single- molecule imaging of quantum-dot-labeled proteins. Mol.Cell 37, 702-713.

Kainov, D. E., Mancini, E. J., Telenius, J., Lisai, J., Grimes, J. M., Bamford, D. H., Stuart, D. I., Tuma, R., 2008. Structural basis of mechanochemical coupling in a hexameric molecular motor. Journal of Biological Chemistry 283, 3607-3617.

Lee, C. S., Guo, P., 1994. A highly sensitive system for the *in vitro* assembly of bacteriophage phi29 of *Bacillus subtilis*. Virology 202, 1039-1042.

Lee, T. J., Guo, P., 2006. Interaction of gp16 with pRNA and DNA for genome packaging by the motor of bacterial virus phi29. J.Mol Biol. 356, 589-599.

Lee, T. J., Zhang, H., Chang, C. L., Savran, C., Guo, P., 2009. Engineering of the fluorescent-energy-conversion arm of phi29 DNA packaging motor for single-molecule studies. Small 5, 2453-2459.

Lee, T. J., Zhang, H., Liang, D., Guo, P., 2008. Strand and nucleotide-dependent ATPase activity of gp16 of bacterial virus phi29 DNA packaging motor. Virology 380, 69-74.

Lowe, J., Ellonen, A., Allen, M. D., Atkinson, C., Sherratt, D. J., Grainge, I., 2008. Molecular mechanism of sequence-directed DNA loading and translocation by FtsK. Mol.Cell 31, 498-509.

Maluf, N. K., Feiss, M., 2006. Virus DNA translocation: progress towards a first ascent of mount pretty difficult. Mol Microbiol. 61, 1-4.

Maluf, N. K., Gaussier, H., Bogner, E., Feiss, M., Catalano, C. E., 2006. Assembly of Bacteriophage Lambda Terminase into a Viral DNA Maturation and Packaging Machine. Biochemistry. 45, 15259-15268.

Martin, A., Baker, T. A., Sauer, R. T., 2005. Rebuilt AAA + motors reveal operating principles for ATP-fuelled machines. Nature 437, 1115-1120.

Massey, T. H., Mercogliano, C. P., Yates, J., Sherratt, D. J., Lowe, J., 2006. Double-stranded DNA translocation: structure and mechanism of hexameric FtsK. Mol.Cell 23, 457-469.

Mastrangelo, I. A., Hough, P. V., Wall, J. S., Dodson, M., Dean, F. B., Hurwitz, J., 1989. ATP-dependent assembly of double hexamers of SV40 T antigen at the viral origin of DNA replication. Nature 338, 658-662.

Mayanagi, K., Kiyonari, S., Saito, M., Shirai, T., Ishino, Y., Morikawa, K., 2009. Mechanism of replication machinery assembly as revealed by the DNA ligase-PCNA-DNA complex architecture. Proc.Natl.Acad.Sci.U.S.A 106, 4647-4652.

McNally, R., Bowman, G. D., Goedken, E. R., O'Donnell, M., Kuriyan, J., 2010. Analysis of the role of PCNA-DNA contacts during clamp loading. BMC.Struct.Biol. 10, 3.

Moffitt, J. R., Chemla, Y. R., Aathavan, K., Grimes, S., Jardine, P. J., Anderson, D. L., Bustamante, C., 2009. Intersubunit coordination in a homomeric ring ATPase. Nature 457, 446-450.

Moll, D., Guo, P., 2007. Grouping of Ferritin and Gold Nanoparticles Conjugated to pRNA of the Phage phi29 DNA-packaging motor. J Nanosci and Nanotech (JNN) 7, 3257-3267.

Morais, M. C., Koti, J. S., Bowman, V. D., Reyes-Aldrete, E., Anderson D, Rossman, M. G., 2008. Defining molecular and domain boundaries in the bacteriophage phi29 DNA packaging motor. Structure 16, 1267-1274.

Morais, M. C., Tao Y, Olsen, N. H., Grimes, S., Jardine, P. J., Anderson, D., Baker TS, Rossmann, M. G., 2001. Cryoelectron-Microscopy Image Reconstruction of Symmetry Mismatches in Bacteriophage phi29. Journal of Structural Biology 135, 38-46.

Morita, M., Tasaka, M., Fujisawa, H., 1995b. Structural and functional domains of the large subunit of the bacteriophage T3 DNA packaging enzyme: importance of the C-terminal region in prohead binding. J.Mol.Biol. 245, 635-644.

Morita, M., Tasaka, M., Fujisawa, H., 1993. DNA packaging ATPase of bacteriophage T3. Virology 193, 748-752.

Morita, M., Tasaka, M., Fujisawa, H., 1995a. Analysis of the fine structure of the prohead binding domain of the packaging protein of bacteriophage T3 using a hexapeptide, an analog of a prohead binding site. Virology 211, 516-524.

Mueller-Cajar, O., Stotz, M., Wendler, P., Hartl, F. U., Bracher, A., Hayer-Hartl, M., 2011. Structure and function of the AAA+ protein CbbX, a red-type Rubisco activase. Nature 479, 194-199.

Niedenzu, T., Roleke, D., Bains, G., Scherzinger, E., Saenger, W., 2001. Crystal structure of the hexameric replicative helicase RepA of plasmid RSF1010. J.Mol.Biol. 306, 479-487.

Parsons, C. A., Stasiak, A., Bennett, R. J., West, S. C., 1995. Structure of a multisubunit complex that promotes DNA branch migration. Nature 374, 375-378.

Putnam, C. D., Clancy, S. B., Tsuruta, H., Gonzalez, S., Wetmur, J. G., Tainer, J. A., 2001. Structure and mechanism of the RuvB Holliday junction branch migration motor. J.Mol.Biol. 311, 297-310.

Rao, V. B., Feiss, M., 2008. The Bacteriophage DNA Packaging Motor. Annu.Rev.Genet. 42, 647-681.

Ray, K., Ma, J., Oram, M., Lakowicz, J. R., Black, L. W., 2010. Single-molecule and FRET fluorescence correlation spectroscopy analyses of phage DNA packaging: colocalization of packaged phage T4 DNA ends within the capsid. J.Mol.Biol. 395, 1102-1113.

Ray, K., Sabanayagam, C. R., Lakowicz, J. R., Black, L. W., 2010. DNA crunching by a viral packaging motor: Compression of a procapsid-portal stalled Y-DNA substrate. Virology 398, 224-232.

Roy, A., Bhardwaj, A., Cingolani, G., 2011. Crystallization of the nonameric small terminase subunit of bacteriophage P22. Acta Crystallographica Section F-Structural Biology and Crystallization Communications 67, 104-110.

Sabanayagam, C. R., Oram, M., Lakowicz, J. R., Black, L. W., 2007. Viral DNA packaging studied by fluorescence correlation spectroscopy. Biophys.J 93, L17-L19.

Schwartz, C., De Donatis, G. M., Fang, H., Guo, P. The ATPase of the phi29 DNA-packaging motor is a member of the hexameric AAA+ superfamily. Virology . 2013.

Schwartz, C., Fang, H., Huang, L., Guo, P., 2012. Sequential action of ATPase, ATP, ADP, Pi and dsDNA in procapsid-free system to enlighten mechanism in viral dsDNA packaging. Nucleic Acids Research 40, 2577-2586.

Serwer, P., 2003. Models of bacteriophage DNA packaging motors. J Struct.Biol 141, 179-188.

Serwer, P., 2010. A Hypothesis for Bacteriophage DNA Packaging Motors. Viruses-Basel 2, 1821-1843.

Shibata, H., Fujisawa, H., Minagawa, T., 1987. Early events in a defined *in vitro* system for packaging of bacteriophage T3 DNA. Virology 159, 250-258.

Shu, D., Shu, Y., Haque, F., Abdelmawla, S., Guo, P., 2011. Thermodynamically stable RNA three-way junctions as platform for constructing multifuntional nanoparticles for delivery of therapeutics. Nature Nanotechnology 6, 658-667.

Shu, D., Guo, P., 2003a. A Viral RNA that binds ATP and contains an motif similar to an ATP-binding aptamer from SELEX. J.Biol.Chem. 278(9), 7119-7125.

Shu, D., Guo, P., 2003b. Only one pRNA hexamer but multiple copies of the DNA-packaging protein gp16 are needed for the motor to package bacterial virus phi29 genomic DNA. Virology 309(1), 108-113.

Shu, D., Zhang, H., Jin, J., Guo, P., 2007. Counting of six pRNAs of phi29 DNA-packaging motor with customized single molecule dual-view system. EMBO Journal **26**, 527-537.

Simpson, A. A., Tao, Y., Leiman, P. G., Badasso, M. O., He, Y., Jardine, P. J., Olson, N. H., Morais, M. C., Grimes, S., Anderson, D. L., Baker, T. S., Rossmann, M. G., 2000. Structure of the bacteriophage phi29 DNA packaging motor. Nature 408, 745-750.

Story, R. M., Steitz, T. A., 1992. Structure of the rec-A protein-ADP Complex. Nature 355.

Trottier, M., Guo, P., 1997. Approaches to determine stoichiometry of viral assembly components. Journal of Virology 71, 487-494.

Wang, F., Mei, Z., Qi, Y., Yan, C., Hu, Q., Wang, J., Shi, Y., 2011. Structure and mechanism of the hexameric MecA-ClpC molecular machine. Nature 471, 331-335.

Willows, R. D., Hansson, A., Birch, D., Al-Karadaghi, S., Hansson, M., 2004. EM single particle analysis of the ATP-dependent BchI complex of magnesium chelatase: an AAA(+) hexamer. Journal of Structural Biology 146, 227-233.

Xiao, F., Zhang, H., Guo, P., 2008. Novel mechanism of hexamer ring assembly in protein/RNA interactions revealed by single molecule imaging. Nucleic Acids Res 36 (20), 6620-6632.

Xiao, F., Demeler, B., Guo, P., 2010. Assembly Mechanism of the Sixty-Subunit Nanoparticles via Interaction of RNA with the Reengineered Protein Connector of phi29 DNA-Packaging Motor. ACS Nano. 4, 3293-3301.

Yu, J., Moffitt, J., Hetherington, C. L., Bustamante, C., Oster, G., 2010. Mechanochemistry of a viral DNA packaging motor. J.Mol.Biol. 400, 186-203.

Zhang, F., Lemieux, S., Wu, X., St.-Arnaud, S., McMurray, C. T., Major, F., Anderson, D., 1998. Function of hexameric RNA in packaging of bacteriophage phi29 DNA in vitro. Molecular Cell 2, 141-147.

Zhang, H., Schwartz, C., De Donatis, G. M., Guo, P., 2012. Hexameric viral DNA packaging motor using a "Push through a one-way valve" mechanism. Adv.Virus Res 83, 415-465.

Zhang, H., Endrizzi, J. A., Shu, Y., Haque, F., Guo, P., Chi, Y. I., 2012. The 3WJ core crystal structure reveals divalent ion-promoted thermostability and functional assembly of the phi29 hexameric motor pRNA. RNA Submitted.

Zhao, Z., Khisamutdinov, E., Schwartz, C., Guo, P., 2013. Mechanism of one-way traffic of the hexameric DNA Translocation motor by means of anti-parallel helixes and four lysine layers. ACS Nano.